










Research Article

Mitochondrial-Protective Effects of R-Phenibut after Experimental Traumatic Brain Injury

Einars Kupats ^{1,2}, Gundega Stelfa ^{1,3}, Baiba Zvejniece ¹, Solveiga Grinberga ¹,
Edijs Vavers ¹, Marina Makrecka-Kuka ¹, Baiba Svalbe ¹, Liga Zvejniece ¹,
and Maija Dambrova ^{1,4}

¹Latvian Institute of Organic Synthesis, Riga, Latvia

²Department of Neurology and Neurosurgery, Riga Stradins University, Riga, Latvia

³Latvia University of Life Sciences and Technologies, Jelgava, Latvia

⁴Department of Pharmaceutical Chemistry, Riga Stradins University, Riga, Latvia

Correspondence should be addressed to Einars Kupats; einars.kupats@farm.osi.lv

Received 15 July 2020; Revised 24 September 2020; Accepted 3 November 2020; Published 21 November 2020

Academic Editor: Luciano Saso

Copyright © 2020 Einars Kupats et al. This is an open access article distributed under the Creative Commons Attribution License, which permits unrestricted use, distribution, and reproduction in any medium, provided the original work is properly cited.

Altered neuronal Ca^{2+} homeostasis and mitochondrial dysfunction play a central role in the pathogenesis of traumatic brain injury (TBI). R-Phenibut ((3R)-phenyl-4-aminobutyric acid) is an antagonist of the $\alpha_2\delta$ subunit of voltage-dependent calcium channels (VDCC) and an agonist of gamma-aminobutyric acid B (GABA-B) receptors. The aim of this study was to evaluate the potential therapeutic effects of R-phenibut following the lateral fluid percussion injury (latFPI) model of TBI in mice and the impact of R- and S-phenibut on mitochondrial functionality *in vitro*. By determining the bioavailability of R-phenibut in the mouse brain tissue and plasma, we found that R-phenibut (50 mg/kg) reached the brain tissue 15 min after intraperitoneal (i.p.) and peroral (p.o.) injections. The maximal concentration of R-phenibut in the brain tissues was 0.6 $\mu\text{g/g}$ and 0.2 $\mu\text{g/g}$ tissue after i.p. and p.o. administration, respectively. Male Swiss-Webster mice received i.p. injections of R-phenibut at doses of 10 or 50 mg/kg 2 h after TBI and then once daily for 7 days. R-Phenibut treatment at the dose of 50 mg/kg significantly ameliorated functional deficits after TBI on postinjury days 1, 4, and 7. Seven days after TBI, the number of Nissl-stained dark neurons (N-DNs) and interleukin-1beta (IL-1 β) expression in the cerebral neocortex in the area of cortical impact were reduced. Moreover, the addition of R- and S-phenibut at a concentration of 0.5 $\mu\text{g/ml}$ inhibited calcium-induced mitochondrial swelling in the brain homogenate and prevented anoxia-reoxygenation-induced increases in mitochondrial H_2O_2 production and the $\text{H}_2\text{O}_2/\text{O}$ ratio. Taken together, these results suggest that R-phenibut could serve as a neuroprotective agent and promising drug candidate for treating TBI.

1. Introduction

Traumatic brain injury (TBI) is a leading cause of mortality and disability among trauma-related injuries [1]. TBI can result in temporary, long-term, and even life-long physical, cognitive, and behavioural problems [2, 3]. Therefore, there is an increased need for effective pharmacological approaches for treating patients with TBI. Phenibut, a nootropic prescription drug with anxiolytic activity, is used in clinical practice in Eastern European countries for the treatment of anxiety, tics, stuttering, insomnia, dizziness, and alcohol abstinence [4, 5]. R-Phenibut ((3R)-phenyl-4-aminobutyric

acid), which is one of the optical isomers of phenibut, binds to gamma-aminobutyric acid B (GABA-B) receptors and the $\alpha_2\delta$ subunit of voltage-dependent calcium channels (VDCC), while S-phenibut binds only to the $\alpha_2\delta$ subunit of VDCC [6–8]. Our previous studies have shown that R-phenibut treatment significantly decreased the brain infarct size and increased brain-derived neurotrophic factor and vascular endothelial growth factor gene expression in damaged brain tissue in an experimental stroke model [9]. The similarity of the pathogenic mechanisms of TBI and cerebral ischaemia indicate that therapeutic strategies that are successful in treating one may also be beneficial in treating the other [10].

Treatment options for TBI are limited due to its complex pathogenesis and the heterogeneity of its presentation, which includes haematomas, contusions, hypoxia, and vascular, axonal, and other types of central nervous system injuries [11, 12]. Among the processes that impact TBI, the generation of reactive oxygen species (ROS) by mitochondria occurs within the first minutes after TBI and thus leads to the disruption of calcium ion (Ca^{2+}) homeostasis, which is the “final common pathway” for toxic cellular degradation [13, 14]. Maintaining regional neuronal Ca^{2+} homeostasis and mitochondrial function is crucial to prevent secondary neuronal injury [15, 16]. Thus, mitochondrial-targeted drugs and drugs acting on specific intracellular Ca^{2+} signalling pathways or subcellular components show promise as therapeutic interventions for TBI [17, 18]. In fact, upregulation of the neuronal calcium channel $\alpha_2\delta$ subunit modulates the activation of mitochondrial Ca^{2+} buffering in pathological conditions [19]. There is also evidence that GABA-B receptor agonists provide neuroprotection against N-methyl-D-aspartate-induced neurotoxicity mediated by the mitochondrial permeability transition pore [20]. Since both isomers of phenibut bind to the $\alpha_2\delta$ subunit of VDCC and only R-phenibut binds to the GABA-B receptor, these both isomers could be used to specify the possible molecular mechanisms of phenibut in different experimental models.

This is the first investigation of the potential therapeutic effects of R-phenibut following TBI in mice. In addition, to evaluate possible molecular mechanisms underlying the actions of R-phenibut against anoxia-reoxygenation-induced mitochondrial damage, the effects on mitochondrial functionality were evaluated in an *in vitro* model of anoxia-reoxygenation and compared for R- and S-phenibut.

2. Materials and Methods

2.1. Animals and Treatment. Forty-eight Swiss-Webster male mice (25–40 g; Laboratory Animal Centre, University of Tartu, Tartu, Estonia) were used in a lateral fluid percussion injury (latFPI) model of TBI [21, 22]. Additionally, 6 Swiss-Webster male mice were used for the preparation of brain homogenate and the isolation of brain mitochondria for *in vitro* assays. Forty-two ICR male mice (Laboratory Animal Breeding Facility, Riga Stradins University, Latvia) were used in a pharmacokinetic study. All animals were housed under standard conditions (21–23°C, 12 h light-dark cycle) with unlimited access to standard food (Lactamin AB, Mjölby, Sweden) and water in an individually ventilated cage housing system (Allentown Inc., Allentown, New Jersey, USA). Each cage contained bedding consisting of Eco-Pure™ Shavings wood chips (Datesand, Cheshire, UK), nesting material, and wooden blocks from TAPVEI (TAPVEI, Paekna, Estonia). For enrichment, a transparent tinted (red) nontoxic durable polycarbonate safe harbour mouse retreat (AnimaLab, Poznan, Poland) was used. The mice were housed with up to 5 mice per standard cage (38 × 19 × 13 cm). All studies involving animals were reported in accordance with the ARRIVE guidelines [23, 24]. The experimental procedures were performed in accordance with the guidelines reported in the EU Directive 2010/63/EU and in accordance

with local laws and policies; all procedures were approved by the Latvian Animal Protection Ethical Committee of Food and Veterinary Service in Riga, Latvia.

The dose of R-phenibut was selected based on the previous studies, where pharmacological efficacy was observed in dose-range between 10 and 50 mg/kg, while R-phenibut at doses higher than 100 mg/kg showed sedative and coordination inhibitory effects [6, 8, 9]. Mice were randomly assigned to four experimental groups: sham-operated mice, saline-treated latFPI mice, and latFPI mice that received R-phenibut (JSC Olainfarm, Olaine, Latvia) at a dose of 10 mg/kg or 50 mg/kg. Six mice were excluded because of a dural breach that occurred during surgery (4 mice from the sham-operated, 1 mouse from the control, and 1 mouse from the R-phenibut 50 mg/kg groups), and four mice died immediately after latFPI and were excluded from the study (3 mice from the control and 1 mouse from the R-phenibut 50 mg/kg groups). The final number of included animals per group was as follows: sham-operated mice ($n = 8$), saline-treated latFPI mice (control group, $n = 8$), and latFPI mice that received R-phenibut at a dose of 10 mg/kg ($n = 12$) or 50 mg/kg ($n = 10$). R-Phenibut and saline were initially administered intraperitoneally (i.p.) 2 h after injury and then once daily for an additional 7 days for a total treatment period of 1 week. During the treatment period, the animals were weighed at 0, 1, 2, 4, and 7 days after latFPI between 9:00 and 10:00 am. To avoid the influence of subjective factors on the rating process, all experimental procedures were performed in a blinded fashion.

2.2. Determination of R-Phenibut in the Plasma and Brain Tissue after p.o. and i.p. Administration. The concentrations of R-phenibut in the brain tissue extracts and plasma were measured by ultraperformance liquid chromatography-tandem mass spectrometry (UPLC/MS/MS). To determine the concentration of R-phenibut in the plasma and brain, mice received an i.p. and p.o. R-phenibut at a dose of 50 mg/kg 15 and 30 min and 1, 2, 4, 6, and 24 h ($n = 3$ in each time point) before the plasma and brain tissue collection. The blood and brain samples were prepared as described previously [25]. The chromatographic separation was performed using an ACQUITY UPLC system (Waters, USA) on an ACQUITY UPLC BEH Shield RP18 (1.7 μm , 2.1 × 50 mm) (Waters) with a gradient elution from 5 to 98% acetonitrile in 0.1% formic acid aqueous solution at a flow rate of 0.15 ml/min. The analyte was ionized by electrospray ionization in positive ion mode on a Quattro Micro triple quadrupole mass spectrometer (Waters). The mass spectrometer was set up as follows: capillary voltage of 3.3 kV; source and desolvation temperatures of 120 and 400°C, respectively. Cone voltage was 20 V, and collision energy was 18 eV. R-Phenibut analysis was performed in the MRM mode. Precursor to production transition was $m/z/m/z$ 180.0 → 116.1. Data acquisition and processing were performed using the MassLynx V4.1 and QuanLynxV4.1 software (Waters).

2.3. Lateral Fluid Percussion Injury-Induced Brain Trauma. To induce TBI, the latFPI model was generated as previously described [21, 22] with slight modifications. Mice were

anaesthetized with 4% isoflurane contained in a mixture of oxygen and nitrous oxide (70:30, AGA, Riga, Latvia), and anaesthesia with 2% isoflurane (Chemical Point, Deisenhofen, Germany) was maintained during the surgical procedures using a face mask. The depth of anaesthesia was monitored by a toe pinch using tweezers. Before trauma induction, mice received subcutaneous (s.c.) administration of tramadol (KRKA, Novo Mesto, Slovenia) (10 mg/kg). Eye cream was applied to prevent the eyes from drying out. A midline longitudinal scalp incision was made, and the skull was exposed. A craniectomy that was centred at 2 mm posterior to bregma and 2 mm right of midline was performed using a 3 mm outer-diameter trephine. Any animal noted to have a dural breach was euthanized and excluded from the study. A plastic cap was attached over the craniotomy using dental cement (Fullident, Switzerland), and a moderate severity (1.5 ± 0.2 atm) brain injury was induced with a commercially available fluid percussion device (AmScien Instruments, Richmond, USA). Immediately after the injury, apnoea was noted, and when spontaneous breathing returned, anaesthesia was resumed. The cement and cap were removed, and the skin was sutured using resorbable sutures (6-0, silk). The animal was placed in a separate cage to allow full recovery from anaesthesia. Sham-injured animals were subjected to an identical procedure as the latFPI animals except for the induction of trauma.

2.4. Neurological Severity Score (NSS). The neurobehavioural status of mice was obtained by the NSS using the method described previously [26]. The animals were trained on the NSS beams and equipment prior to the baseline measurements. The general neurological state of mice was evaluated at baseline (day before latFPI) and 1, 4, and 7 days postinjury before the next dose of R-phenibut or saline administration. The NSS consisted of 9 individual clinical parameters, including motor function, alertness, and physiological behaviour tasks. The mice were assessed for the following items: presence of paresis; impairment of seeking behaviour; absence of perceptible startle reflex; inability to get down from a rectangle platform (34×27 cm); inability to walk on 3, 2, and 1 cm wide beams; and inability to balance on a vertical beam of 7 mm width and horizontal round stick of 5 mm diameter for 10 sec. If a mouse showed impairment on one of these items, a value of 1 was added to its NSS score. Thus, higher scores on the NSS indicate greater neurological impairment.

2.5. Tissue Preparation for Histological Analysis. The animals used for histological analysis were randomly selected from each group. Seven days after TBI, the mice were anaesthetized using i.p. administration of ketamine (200 mg/kg) and xylazine (15 mg/kg). The depth of anaesthesia was monitored by a toe pinch using tweezers. Animals were transcardially perfused at a rate of 3 ml/minutes with 0.01 M phosphate-buffered saline (PBS, pH = 7.4) for 5 minutes until the blood was completely removed from the tissue. Perfusion was then performed with 4% paraformaldehyde (PFA) fixative solution for 5-7 minutes until stiffening of the mouse body occurred. After perfusion, the brains were carefully dissected

and postfixed in 4% PFA overnight at 4°C. The brains were cryoprotected with a 10-20-30% sucrose-PBS gradient for 72 hours. Coronal sections of the brain (20 μ m) were made using a Leica CM1850 cryostat (Leica Biosystems, Buffalo Grove, IL, United States) and mounted on Superfrost Plus microscope slides (Thermo Scientific, Waltham, MA, United States).

2.6. Cresyl Violet (Nissl) Staining and Interleukin-1beta (IL-1 β) Immunofluorescence Staining. Nissl and IL-1 β staining techniques were used to evaluate neuronal cell damage. Nissl-stained dark neurons (N-DNs) indicated the typical morphological change in injured neurons following TBI [27, 28]. The number of N-DNs and cells expressing IL-1 β in the cerebral neocortex in the cortical impact area were determined at day 7 after latFPI. For Nissl staining, coronal frozen sections (20 μ m) of the mouse brain were used. The sections were incubated in graded ethanol solutions (96% ethanol for 3 minutes and 70% ethanol for 3 minutes). After washing with distilled water for 3 minutes, the sections were stained with 0.01% cresyl violet acetate (ACROS organics) solution for 14 minutes. The sections were then washed with distilled water for 3 minutes and dehydrated in ethanol. The stained sections were coverslipped using DPX mounting medium (Sigma-Aldrich, St. Louis, MO, United States).

For IL-1 β staining, the sections were washed once with PBS containing 0.2% Tween 20 for 5 minutes (on a rotary shaker at 250 rpm). The antigen retrieval procedure was performed with 0.05 M Na citrate (pH = 6.0) containing 0.05% Tween 20 for 30 minutes at 85°C. The sections were then washed with PBS (0.2% Tween 20) 3 times for 5 minutes each. Protein blocking was performed using 5% BSA solution, and the sections were incubated for 1 hour at room temperature. The sections were washed with PBS (0.2% Tween 20) 3 times for 5 minutes each. The slices were incubated with primary antibody against anti-IL-1 β (1:1000; Abcam, Cat# ab9722) for 16 h at +4°C. The antibody was diluted in PBS containing 3% BSA and 0.3% Triton™ X-100. After incubation with the primary antibody, the sections were washed with PBS (0.2% Tween 20) 4 times for 5 minutes each. The sections were subsequently incubated for 1 h at room temperature with goat anti-rabbit IgG H&L (Alexa Fluor® 488, 1:200; Abcam, Cat# ab150077) diluted in PBS containing 5% BSA. The sections were washed with PBS (0.2% Tween 20) 4 times for 5 minutes each. The stained sections were mounted using Fluoromount™ aqueous mounting medium (Sigma-Aldrich, St. Louis, MO, United States, Cat# F4680) and finally coverslipped. Images were obtained with a Nikon Eclipse TE300 microscope (Nikon Instruments, Tokyo, Japan).

N-DNs were defined as hyperbasophilic neurons with a shrunken morphology. The number of N-DNs per field of vision was calculated in three randomly selected sections at the epicentre of the injury. The number of N-DNs and cells expressing IL-1 β per field of vision were calculated using ImageJ software at 10-fold magnification for N-DNs and at 4-fold magnification for IL-1 β . For analysis of expression of IL-1 β , eight-bit images were generated from the pictures and were cropped to contain the regions of interest. Images

for IL-1 β staining were thresholded to select a specific signal over the background, and the stained area for each region was calculated and used for statistical analysis. Three individual measurements were performed for each sample. The schematic illustration of the brain region was created using BioRender software (<https://biorender.com>).

2.7. Mitochondrial Respiration and H₂O₂ Production Measurements. To evaluate mitochondrial functionality, mouse brain homogenate or isolated brain mitochondria were prepared. Briefly, brain tissues were homogenized 1:20 (*w/v*) in a medium containing 320 mM sucrose, 10 mM Tris, and 1 mM EDTA (pH 7.4). The homogenate was centrifuged at 1000 g for 10 min, and the supernatant was centrifuged at 6200 g for 10 min. The mitochondrial pellet obtained was washed once and resuspended in the isolation medium. Mitochondrial respiration and H₂O₂ production measurements were performed at 37°C using Oxygraph-2k (O2k; Oroboros Instruments, Austria) with O2k-Fluo-Modules in MiR05Cr (110 mM sucrose, 60 mM K-lactobionate, 0.5 mM EGTA, 3 mM MgCl₂, 20 mM taurine, 10 mM KH₂PO₄, 20 mM HEPES, pH 7.1, 0.1% BSA essentially fatty acid free, and creatine 20 mM). H₂O₂ flux (ROS flux) was measured simultaneously with respirometry in the O2k-fluorometer using the H₂O₂-sensitive probe Ampliflu™ Red (AmR) [29, 30]. 10 μ M AmR, 1 U/ml horse radish peroxidase (HRP), and 5 U/ml superoxide dismutase (SOD) were added to the chamber. H₂O₂ detection is based on the conversion of AmR into the fluorescent resorufin. Calibrations were performed with H₂O₂ added at 0.1 μ M step. H₂O₂ flux was corrected for background (AmR slope before addition of sample). H₂O₂/O flux ratio (%) was calculated as H₂O₂ flux/(0.5 O₂ flux).

2.8. In Vitro Anoxia-Reoxygenation Model. Mitochondrial functionality after anoxia-reoxygenation was determined in mouse brain tissue homogenate prepared as described previously [31]. To induce anoxia maximal respiration rate, the sample was stimulated by the addition of substrates, pyruvate + malate (5 + 2 mM), succinate (10 mM), and ADP (5 mM), and preparation was left to consume all O₂ in the respiratory chamber (within 10–20 min), thereby entering into an anoxic state [32]. 15 minutes after anoxia, the vehicle or R-phenibut (0.5 μ g/ml) was added to the chamber and O₂ was reintroduced to the chamber by opening the chamber to achieve reoxygenation. After 8 minutes of reoxygenation, the chamber was closed and O₂ flux was monitored for additional 2 minutes. At the end of the experiment, antimycin A (2.5 μ M) was added to determine residual oxygen consumption (ROX).

2.9. Substrate-Uncoupler-Inhibitor Titration (SUIT) Protocol. To determine the effect of R-phenibut on mitochondrial electron transfer system functionality, mitochondria were isolated from mouse brain as described previously, and mitochondrial respiration and H₂O₂ production measurements were performed in the presence or absence of R-phenibut at 0.5 μ g/ml concentration [30]. In addition, effects of S-phenibut (0.5 μ g/ml) were tested to determine whether

the effects of R-phenibut in mitochondria involve the GABA-B receptor or the $\alpha_2\delta$ subunit of VDCC. Pyruvate and malate (5 mM and 2 mM, respectively) were used to determine N-pathway complex I (CI) linked LEAK (L) respiration. ADP was added at 5 mM concentration to determine oxidative phosphorylation-dependent respiration (OXPHOS state, P). Then, glutamate (10 mM) was added as an additional substrate for N-pathway. Succinate (10 mM, complex II (CII) substrate) was added to reconstitute convergent NS-pathway CI&II-linked respiration. Titrations with the uncoupler CCCP (0.5–1 μ M steps) were performed to determine the electron transfer system (ETS) capacity. Rotenone (0.5 μ M, inhibitor of complex I) was added to determine the CII-linked OXPHOS capacity. Then, antimycin A (2.5 μ M, inhibitor of complex III) was added to evaluate residual (non-mitochondrial) oxygen consumption (ROX). Oxygen fluxes were compared after correction for ROX.

2.10. Ca²⁺-Induced Mitochondrial Swelling Measurement. Swelling of isolated brain mitochondria was assessed by measuring changes in absorbance at 540 nm as described previously with slight modifications [33–35]. Mitochondria (0.125 mg/ml) were preincubated with R- or S- phenibut at a concentration of 0.5 μ g/ml for 15 min in a buffer containing 120 mM KCl, 10 mM Tris, 5 mM KH₂PO₄ pH 7.4, and pyruvate (5 mM), malate (2 mM), and ADP (5 mM) as substrates. R- and S-enantiomers of phenibut were used to determine whether the effects of R-phenibut on Ca²⁺-induced mitochondrial swelling involve the GABA-B receptor or the $\alpha_2\delta$ subunit of VDCC. Swelling was induced by the addition of 200 μ M CaCl₂, and changes in absorbance were monitored for 10 min. All experiments were performed at 37°C.

2.11. Statistical Analysis. All results are expressed as the mean \pm S.E.M or S.D. (for mitochondrial studies). Health outcomes, animal behaviour, and Ca²⁺-induced mitochondrial swelling were analysed using two-way repeated-measures analysis of variance (ANOVA). Dunnett's post hoc test was performed when appropriate. The histological data and mitochondrial functionality were evaluated by one-way ANOVA. Whenever the analysis of variance indicated a significant difference, further multiple comparisons were made using Tukey's multiple comparison test as the post hoc test. *p* values less than 0.05 were considered to be significant. The statistical calculations were performed using the GraphPad Prism software package (GraphPad Software, Inc., La Jolla, California, USA).

The sample size calculations for latFPI-induced brain trauma were based on the effects of R-phenibut in our previous experiments. For example, it was calculated that R-phenibut demonstrates a medium effect in the ET-1-induced middle cerebral artery occlusion model [9] and a large effect in the formalin-induced paw-licking test [6]. Through a power calculation (using G-power software) for a two-way ANOVA test (repeated measures), four-group comparison, four measurements per group (0, 1, 4, and 7 days after TBI) with $\alpha = 0.05$, a power of 80%, and a standardized effect size Cohen's *f* = 0.5, a total sample size of 8 mice per group was deemed sufficient. Since TBI-induced

brain trauma can result in death of some animals, our sample size of $n = 12$ would allow identifying smaller differences, with the same statistical power, for the same significance level.

3. Results

3.1. R-Phenibut Crosses the Blood-Brain Barrier. As shown in Figure 1(a), R-phenibut in plasma could be detected 15 min after a single i.p. and p.o. injection. The maximal concentrations of R-phenibut in the plasma were observed 15 min after the i.p. injection and 30 min after the p.o. administration (Figure 1(a)). The maximal concentration of R-phenibut in the plasma after the i.p. injection was $16.8 \mu\text{g/ml}$; at the same time, the maximal concentration of R-phenibut in the plasma after the p.o. injection was $24 \mu\text{g/ml}$ (see Figure 1(a)). R-Phenibut in the plasma was not detected 24 h after both the i.p. and p.o. injections. R-Phenibut in the brain tissue extracts was detected already 15 min after a single i.p. and p.o. injection (Figure 1(b)). The maximal concentrations of R-phenibut in the brain tissues were $0.64 \mu\text{g/g}$ and $0.17 \mu\text{g/g}$ tissue after the i.p. and p.o. injections, respectively (Figure 1(a)). The maximal concentrations of R-phenibut in the brain tissues were observed 15 min after i.p. injection and 60 till 240 min after p.o. administration. 24 h after both the i.p. and p.o. injections, R-phenibut in the brain tissues was $0.02 \mu\text{g/g}$ and $0.012 \mu\text{g/g}$, respectively.

3.2. Health Outcome Monitoring after latFPI. The body weight of the sham group animals was not decreased at 1, 2, 4, and 7 days after TBI. A two-way repeated-measures ANOVA showed a significant interaction between time and treatment ($F_{(12,118)} = 4.6$, $p < 0.0001$) and main effects of time ($F_{(1,4,42.7)} = 25.7$, $p < 0.0001$) and treatment ($F_{(3,34)} = 6.7$, $p = 0.0011$). The control group animals lost significantly more weight after TBI than the sham-operated group animals ($p < 0.05$). Treatment with R-phenibut at both doses had no effect on weight loss compared to weight loss in the control group (Figure 2).

3.3. R-Phenibut Treatment Improved Neurological Status after TBI. TBI induced significant functional deficits in control mice compared with sham-operated mice ($p < 0.0001$). The average NSS in the control group was 6.1 ± 0.4 , 5.3 ± 0.3 , and 5.0 ± 0.6 on postinjury days 1, 4, and 7, respectively. The average NSS score between baseline value and the first day postcraniotomy in the sham-operated group was significantly higher ($p < 0.01$). There was a significant time \times treatment interaction observed between groups (two-way repeated-measures ANOVA: ($F_{(9,102)} = 5.7$, $p < 0.0001$) for time \times treatment interaction; ($F_{(3,34)} = 22.2$, $p < 0.0001$) for treatment; ($F_{(2,7,92)} = 161.8$, $p < 0.0001$) for time; Figure 3). R-Phenibut treatment at a dose of 50 mg/kg significantly ameliorated functional deficits by 28%, 25%, and 30% after TBI on postinjury days 1, 4, and 7, respectively ($p < 0.05$; Figure 3).

3.4. R-Phenibut Treatment Reduced Early Neuronal Cell Death and Neuroinflammation in the Brain Cortex after TBI. To assess histopathological changes in the ipsilateral

brain site, N-DNs and cells expressing IL-1 β (Figure 4) were quantified in the sham-operated, control, and R-phenibut treatment groups 7 days after TBI. N-DNs and IL-1 β -expressing cells were found in the ipsilateral hemisphere of control group animals (Figures 4(a) and 4(b)). Histological analysis showed that R-phenibut treatment at a dose of 50 mg/kg significantly reduced the number of N-DNs and cells expressing IL-1 β in the neocortex after TBI ($p < 0.05$). Significant differences were found in the N-DNs and IL-1 β -positive cell numbers in the ipsilateral cortex around the lesion site between the control group (9.1 ± 6.4 /per field of vision for N-DNs and 379 ± 82 /per field of vision for IL-1 β -expressing cells) and the R-phenibut treatment group at a dose of 50 mg/kg (3.0 ± 1.9 /per field of vision for N-DNs and 246 ± 31 /per field of vision for IL-1 β -expressing cells; $p < 0.05$; Figures 4(d) and 4(e)). There was no statistically significant difference between the control group and the R-phenibut treatment group at the dose of 10 mg/kg. No N-DNs were observed in the sham-operated mice.

3.5. R-Phenibut Protects Brain Mitochondria against Anoxia-Reoxygenation Damage. To determine whether R-phenibut-induced neuroprotection could be a result of the preservation of mitochondrial functionality, ROS production and the mitochondrial respiration rate were assessed after anoxia-reoxygenation *in vitro*. To better mimic the conditions observed *in vivo*, R-phenibut at the concentration of $0.5 \mu\text{g/ml}$ was added to the chamber immediately before reoxygenation. Anoxia-reoxygenation induced 33% and 59% increases in the H_2O_2 production rate and the $\text{H}_2\text{O}_2/\text{O}$ ratio, respectively (Figure 5). R-Phenibut treatment significantly decreased the anoxia-reoxygenation-induced increase in the H_2O_2 production rate and the $\text{H}_2\text{O}_2/\text{O}$ ratio ($p < 0.05$).

3.6. R-Phenibut Reduces ROS Production and Attenuates Ca^{2+} -Induced Mitochondrial Swelling. To determine whether the protective effect of R-phenibut is related to its direct action on mitochondria, measurements of mitochondrial respiration, ROS production, and Ca^{2+} -induced swelling were performed in isolated mouse brain mitochondria in the presence or absence of the compounds. As seen in Figure 6, R-phenibut and S-phenibut at $0.5 \mu\text{g/ml}$ did not induce any changes in the mitochondrial respiration rate (Figure 6(a)), while H_2O_2 production and the $\text{H}_2\text{O}_2/\text{O}$ ratio (Figures 6(b) and 6(c)) were significantly decreased by 31-53% in the LEAK and OXPHOS states. These results show that R-phenibut and S-phenibut reduce ROS production without affecting the mitochondrial electron transfer system capacities, indicating the improvement of mitochondrial coupling. In addition, both R- and S-phenibut attenuated calcium-induced brain mitochondrial swelling (two-way repeated-measures ANOVA: main effect of treatment ($F_{(40,360)} = 4.576$, $p < 0.0001$), time ($F_{(2,611,46.99)} = 104.5$, $p < 0.0001$), and interaction between treatment and time ($F_{(40,360)} = 4.576$, $p < 0.0001$); Figure 6(d)).

Thus, the phenibut treatment-induced protection of mitochondria against anoxia-reoxygenation could be due to a reduction in ROS production and the modulation of Ca^{2+} signalling.

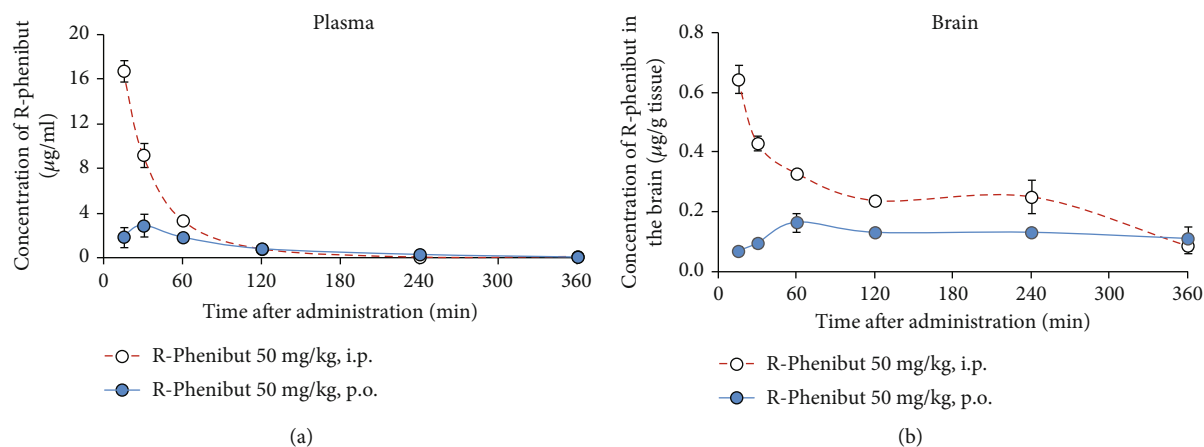


FIGURE 1: The concentration of R-phenibut in the mouse plasma and brain tissue after a single administration. Mice received an i.p. and p.o. injection of R-phenibut at a dose of 50 mg/kg. The amount of compound in the plasma (a) and brain tissue extracts (b) was measured 15 and 30 min and 1, 2, 4, and 6 h after R-phenibut administration ($n = 3$). Values are represented as the mean \pm S.E.M..

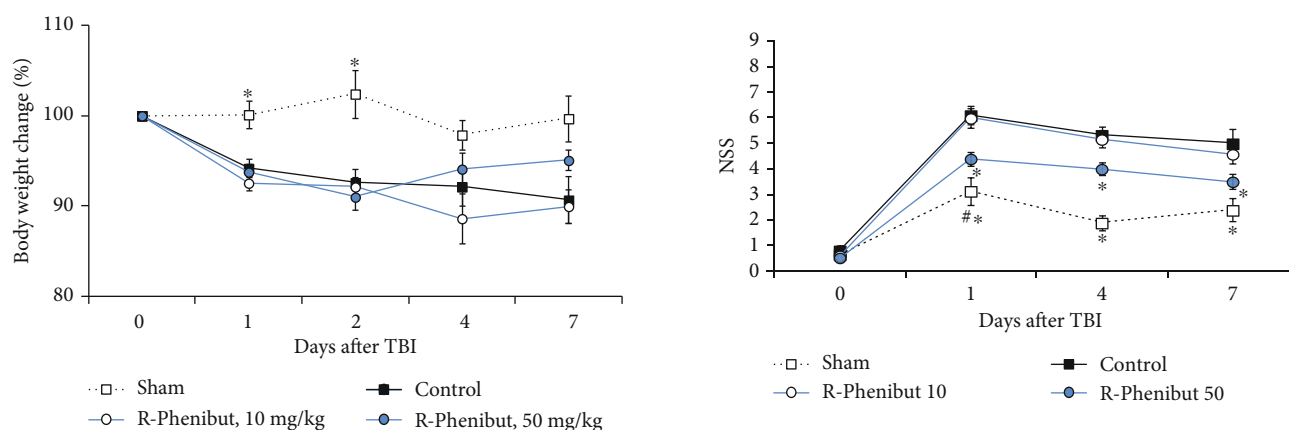


FIGURE 2: Body weight changes of the sham-operated, control, and R-phenibut treatment groups. Mice were weighed before and 1, 2, 4, and 7 days after latFPI. Data are expressed as the percentage change in body weight relative to the initial body weight of each animal (%). Data are shown as the mean \pm S.E.M. ($n = 8 - 12$). *Indicates a significant difference compared to the sham-operated group (two-way repeated-measures ANOVA followed by Dunnett's multiple comparison test; $*P < 0.05$).

4. Discussion

In the current study, we examined the effects of R-phenibut treatment on brain trauma induced by latFPI. For the first time, we showed that R-phenibut could be detected in the mouse brain 15 min after a single p.o. or i.p. injection and found in brain extracts even 24 h after the administration. The present study confirms that R-phenibut, which is an antagonist of the $\alpha_2\delta$ subunit of VDCC and an agonist of GABA-B receptors, improves sensorimotor functional outcomes and significantly ameliorates brain damage and neuronal death in the acute phase after TBI via mechanisms related to Ca^{2+} homeostasis and oxidative stress.

The binding characteristics of R-phenibut were previously investigated using radiolabeled gabapentin that was the first ligand shown to bind to the $\alpha_2\delta_1$ and $\alpha_2\delta_2$ subunits with high affinity ($K_d = 59$ and 153 nM, respectively), while

FIGURE 3: Effects of R-phenibut on the neurological severity score (NSS) after TBI. R-phenibut and saline were initially administered i.p. 2 h after injury and then once daily for an additional 7 days for a total treatment period of 1 week. Data are shown as the mean \pm S.E.M. ($n = 8 - 12$). *Indicates a significant difference compared to the control group; # indicates a significant difference compared to the sham-operated group (two-way repeated-measures ANOVA followed by Dunnett's multiple comparison test; $*P < 0.05$; $\#P < 0.01$).

at the same time demonstrating no binding activity to the $\alpha_2\delta_3$ and $\alpha_2\delta_4$ subunits [36, 37]. The pathologies associated with gene disruption of $\alpha_2\delta_1$ protein include neuropathic pain and cardiac dysfunction, while in case of $\alpha_2\delta_2$ protein, the pathologies are related to epilepsy and cerebellar ataxia [38]. We showed previously that pharmacological activity of R-phenibut is associated with neuropathic pain rather than epilepsy [6]; thus, we could speculate that the effects of R-phenibut are $\alpha_2\delta_1$ protein binding-related.

The $\alpha_2\delta$ subunits of VDCC are widely expressed by excitatory neurons in the cerebral cortex, hippocampus, and other brain regions [39, 40]. Furthermore, the $\alpha_2\delta$ subunits of VDCC have been shown to be involved in processes that are not directly linked to calcium channel function, such as synaptogenesis [41]. Other studies have reported that the administration of VDCC ligands in rodent models of TBI

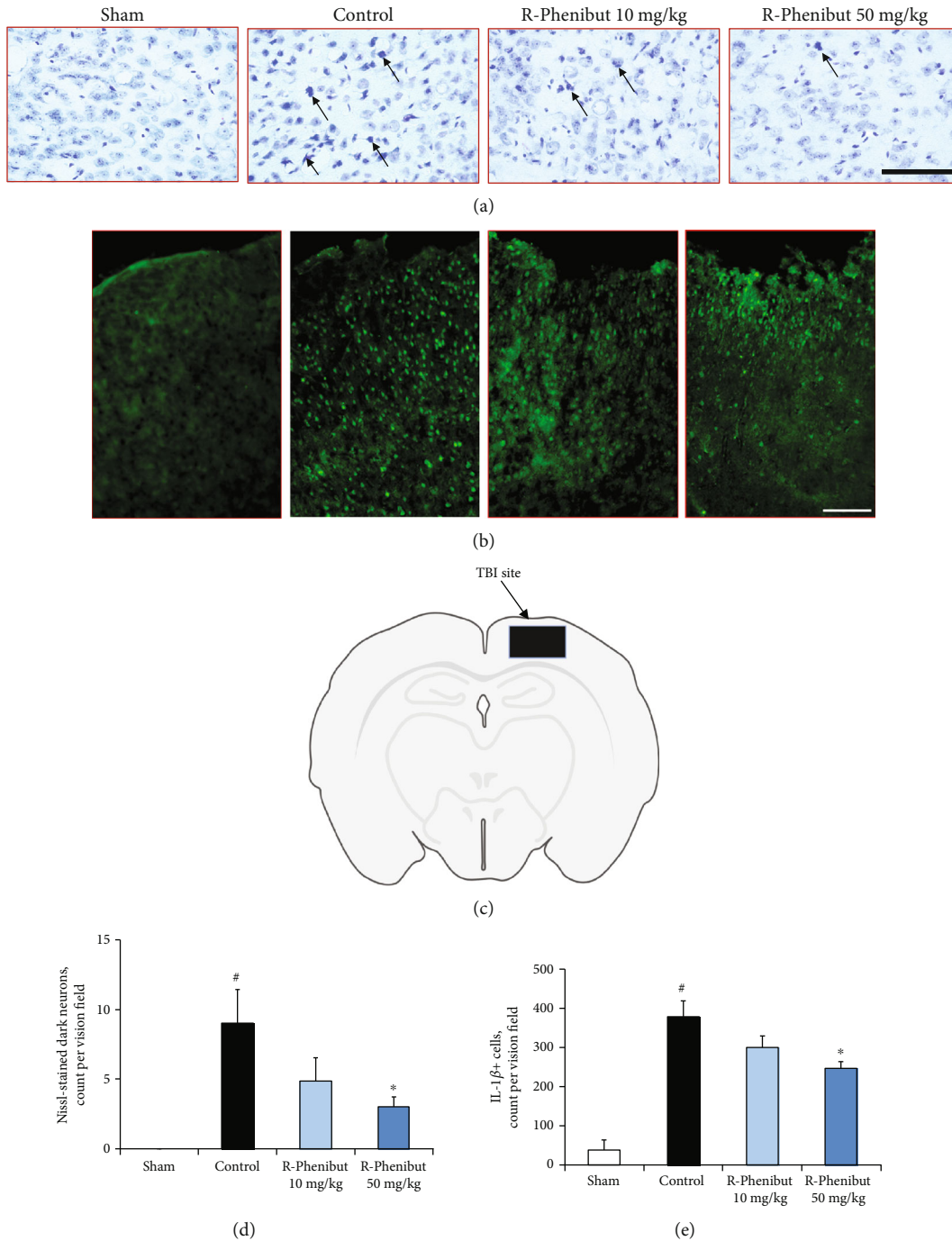


FIGURE 4: Cresyl violet (Nissl) and IL-1 β immunofluorescence staining 7 days post-TBI. (a) Cresyl violet-stained sections of the mouse neocortex ipsilateral to the injury site. R-Phenibut treatment at doses of 10 mg/kg and 50 mg/kg reduced the number of N-DNs. Scale bar = 100 μm . (b) IL-1 β expression based on immunofluorescence staining in the mouse neocortex ipsilateral to the injury site. R-Phenibut treatment at doses of 10 mg/kg and 50 mg/kg reduced the number of IL-1 β -positive cells. Scale bar = 250 μm . (c) Schematic illustration of the brain region indicated in the filled area, which was selected for the quantitative analysis of cell injury. (d) Quantitative assessment of N-DNs in the ipsilateral cortex at postinjury day 7. Data are expressed as the mean \pm S.E.M. ($n = 7$ for the R-phenibut 50 mg/kg group and $n = 6$ for the sham, control, and R-phenibut 10 mg/kg groups). (e) Quantitative assessment of IL-1 β -positive cells in the ipsilateral cortex at postinjury day 7. Data are expressed as the mean \pm S.E.M. ($n = 4$ for the control group and $n = 3$ for the sham, R-phenibut 10 mg/kg, and 50 mg/kg groups). [#]Indicates a significant difference compared to the sham-operated group; ^{*}indicates a significant difference compared to the control group (one-way ANOVA followed by Tukey's multiple comparison test; $*P < 0.05$).

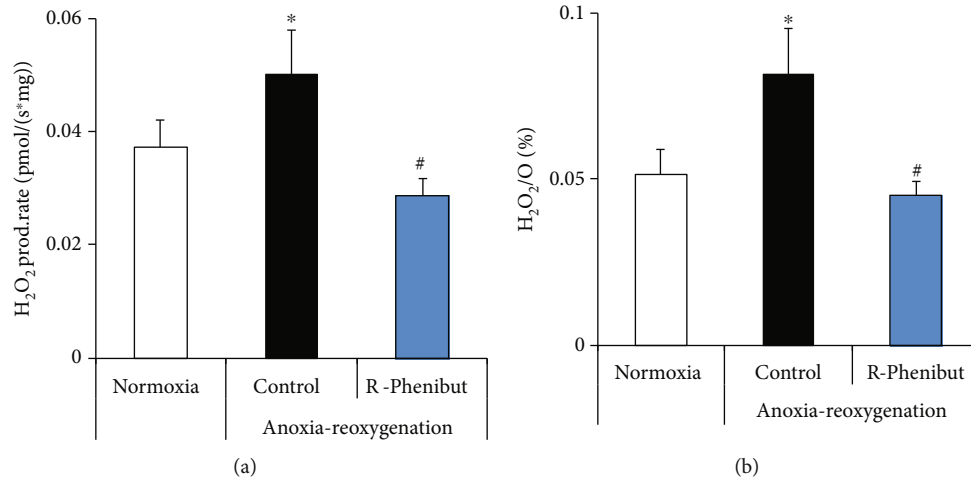


FIGURE 5: The effects of R-phenibut (0.5 $\mu\text{g/ml}$) on ROS production in an *in vitro* anoxia-reoxygenation model. After anoxia-reoxygenation, the H₂O₂ production rate (a) and H₂O₂/O ratio (b) were significantly decreased in the R-phenibut group. The results are presented as the mean \pm S.D. of 6 independent replicates. *Indicates a significant difference compared to normoxia; # indicates a significant difference compared to the anoxia-reoxygenation control group (one-way ANOVA followed by Tukey's multiple comparison test; * $P < 0.05$).

reduced cell death and improved cognitive function [40]. Similar to phenibut, ligands of the $\alpha_2\delta$ subunit of VDCC, such as pregabalin, at a high dose of 60 mg/kg reduce neuronal loss and improve functional outcomes 24 h after trauma in experimental models of TBI [41, 42]. Moreover, pregabalin at a dose of 30 mg/kg has been shown to improve functional recovery and to demonstrate anti-inflammatory and anti-apoptotic effects in a rat model of spinal cord injury [43, 44].

Cytoskeletal protein loss results in altered neuronal morphology after TBI [45, 46]. N-DNs represent a typical pathomorphological change in injured neurons after TBI, showing abnormal basophilia and shrinkage [27, 28]. N-DNs appear in the neocortex immediately after TBI and can be observed even two weeks postinjury [27, 47]. In addition, IL-1 is a major driver of the secondary neuronal injury cascade after TBI [48]. It is involved in the recruitment of other types of immune cells, neuronal apoptosis, and blood-brain barrier disruption after TBI [49–51]. Furthermore, IL-1 β antagonism was shown to be neuroprotective in clinical trials and in rodent models of TBI [52–54]. The present study shows that treatment with R-phenibut at a dose of 50 mg/kg significantly reduced the number of N-DNs and significantly reduced IL-1 β expression in the neocortex after TBI. The histopathological findings of the current study revealed that R-phenibut could attenuate neuronal damage, inflammation, and degeneration.

For the first time, we showed that R-phenibut limits mitochondrial dysfunction in the brain induced by anoxia-reoxygenation. Compared with other types of cells, neurons are endowed with less robust antioxidant defence systems [55]. As mitochondrial dysfunction has been shown to be involved in TBI, perturbations in energy metabolism are likely to contribute to the pathogenesis of TBI [56, 57]. In TBI, oxidative cell damage is caused by an imbalance between the production and accumulation of ROS, in which mitochondria are the major intracellular source of ROS. Accordingly, there is accumulating evidence that antioxidant agents and membrane lipid peroxidation inhibitors, such as tirilazad, U-78517F and U-83836E, are effective in treating

preclinical models of TBI [17]. Mitochondrial-targeted drugs, such as mitoquinone and thymoquinone-containing antioxidants, have been shown to decrease neurological deficits and β -amyloid-induced neurotoxicity after TBI [58, 59]. Meanwhile, the inhibition of ROS production has been shown to inhibit secretion of IL-1 β [60].

Notably, the immunosuppressant drug cyclosporine A, which is an IL-1 β receptor antagonist, has been shown to decrease pathological changes in the brain after TBI by blocking the mitochondrial permeability transition pore [61]. Our results indicate that R-phenibut treatment improves mitochondrial tolerance and thus protects brain energetics against anoxia-reoxygenation damage by reducing ROS production. R-Phenibut treatment reduces ROS production without affecting the mitochondrial electron transfer system capacities, indicating the improvement of mitochondrial coupling. Another study has demonstrated that phenibut has neuroprotective effects *in vitro* but does not possess antioxidant potential [62]. Perfilova et al. recently showed that phenibut can limit heart and brain mitochondrial damage in rats exposed to stress [63].

To determine the molecular mechanisms underlying the actions of R-phenibut against anoxia-reoxygenation-induced mitochondrial damage, the activity of the R- and S-enantiomers of racemic phenibut was compared. We found that both R-phenibut and S-phenibut reduced mitochondrial ROS production and inhibited Ca²⁺-induced mitochondrial swelling. This suggests that the protective effects of R-phenibut in mitochondria do not involve the GABA-B receptor (in contrast to R-phenibut, S-phenibut does not bind to the GABA-B receptor) and might be mediated by the $\alpha_2\delta_1$ subunit of VDCC. It was shown previously that increased intracellular Ca²⁺, as a result of increased activity of $\alpha_2\delta_1$, could be rapidly taken up by mitochondria and subsequently released into the cytoplasm avoiding Ca²⁺ accumulation and maintaining intracellular Ca²⁺ signalling [19]. This could explain why, in the presence of R- and S-phenibut, reduced Ca²⁺-induced mitochondrial swelling was observed. Both R-phenibut and S-phenibut demonstrate mitochondrial-

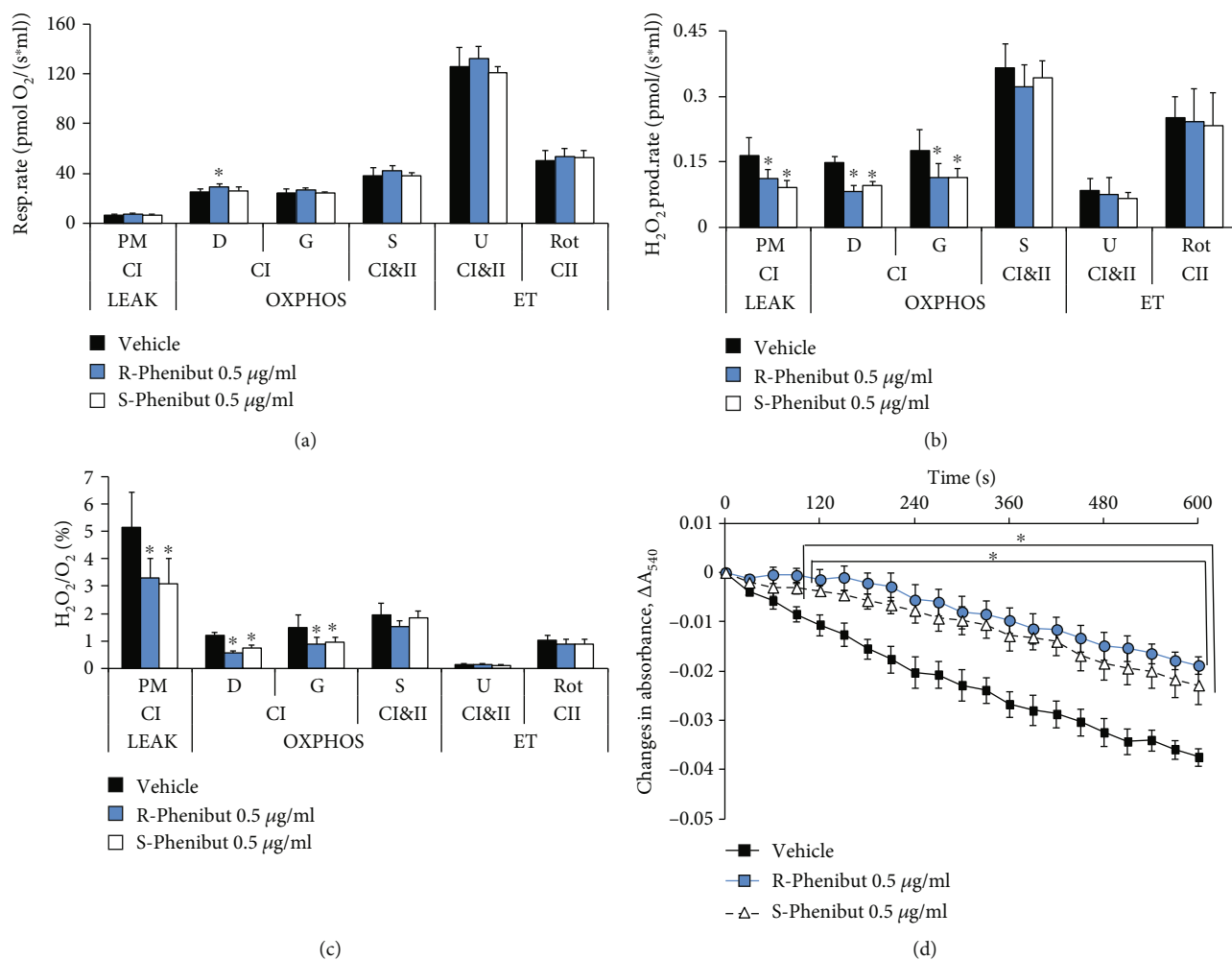


FIGURE 6: The effects of R-phenibut and S-phenibut (0.5 $\mu\text{g/ml}$) on mitochondrial functionality and Ca^{2+} -induced swelling in isolated mouse brain mitochondria. R-Phenibut and S-phenibut did not affect the mitochondrial respiration rate (a) but significantly decreased the H_2O_2 production rate (b) and $\text{H}_2\text{O}_2/\text{O}_2$ ratio (c). The results are presented as the mean \pm S.D. of 5 independent measurements. P: pyruvate; M: malate; D: ADP; G: glutamate; S: succinate; U: uncoupler; Rot: rotenone; CI: complex I; CII: complex II; LEAK: substrate metabolism-dependent state; OXPHOS: oxidative phosphorylation-dependent state; ET: electron transfer capacity state. *Indicates a significant difference compared to the control group (one-way ANOVA followed by Tukey's multiple comparison test, $*P < 0.05$). Both R-phenibut and S-phenibut at a concentration of 0.5 $\mu\text{g/ml}$ significantly attenuated Ca^{2+} -induced swelling (d). The results are presented as the mean \pm S.D. of 7 independent replicates. *Indicates a significant difference compared to the control group (two-way repeated-measures ANOVA followed by Dunnett's multiple comparison test; $*P < 0.05$).

protective properties against anoxia-reoxygenation and Ca^{2+} -induced stress. Since there is no evidence of $\alpha_2\delta$ localization in the mitochondrial membrane, it is possible that compounds could alter Ca^{2+} signalling pathways and protect mitochondria by targeting mitochondrial-specific or mitochondrial-endoplasmic reticulum-associated Ca^{2+} transporters.

Our study has several limitations. One of the limitations of this study is that the level of ROS in mouse brain after treatment of R-phenibut following TBI was not measured. Another limitation is the increase in the NSS score between the baseline value and the first day postcraniotomy in the sham-operated group. The increase of the NSS score in sham-operated mice was reported previously and can be related to the distinct injury caused by craniotomy procedures [64]. Similar to other studies, the NSS score of injured mice showed maximum deficits on postinjury day 1 and

remained elevated at 1, 2, 4, and 7 days after latFPI [64, 65]. A potential limitation of this study is that only male mice were used in experiments.

5. Conclusions

In conclusion, R-phenibut treatment reduces TBI-induced neuronal death and improves functional recovery, suggesting its therapeutic potential. The present study suggests that the neuroprotective properties of phenibut may be mediated by its effects on mitochondrial calcium influx and ROS generation.

Data Availability

The data used to support the findings of this study are available from the corresponding author upon request.

Conflicts of Interest

The authors declare that there is no conflict of interest regarding the publication of this paper.

Acknowledgments

This study was supported by the framework of the EU-ERA-NET NEURON projects TRAINS and CnsAflame.

References

- [1] A. M. Rubiano, N. Carney, R. Chesnut, and J. C. Puyana, "Global neurotrauma research challenges and opportunities," *Nature*, vol. 527, no. 7578, pp. S193–S197, 2015.
- [2] L. J. Carroll, J. D. Cassidy, C. Cancelliere et al., "Systematic review of the prognosis after mild traumatic brain injury in adults: cognitive, psychiatric, and mortality outcomes: results of the international collaboration on mild traumatic brain injury prognosis," *Archives of Physical Medicine and Rehabilitation*, vol. 95, no. 3, pp. S152–S173, 2014.
- [3] M. Majdan, D. Plancikova, A. Brazinova et al., "Epidemiology of traumatic brain injuries in Europe: a cross-sectional analysis," *Lancet Public Health*, vol. 1, no. 2, pp. e76–e83, 2016.
- [4] E. Kupats, J. Vrublevska, B. Zvejniece et al., "Safety and tolerability of the anxiolytic and nootropic drug phenibut: a systematic review of clinical trials and case reports," *Pharmacopsychiatry*, vol. 53, no. 5, pp. 201–208, 2020.
- [5] I. Lapin, "Phenibut (beta-phenyl-GABA): a tranquilizer and nootropic drug," *CNS Drug Reviews*, vol. 7, no. 4, pp. 471–481, 2001.
- [6] L. Zvejniece, E. Vavers, B. Svalbe et al., "R-phenibut binds to the $\alpha 2\text{-}\delta$ subunit of voltage-dependent calcium channels and exerts gabapentin-like anti-nociceptive effects," *Pharmacology, Biochemistry, and Behavior*, vol. 137, pp. 23–29, 2015.
- [7] I. Belozertseva, J. Nagel, B. Valastro, L. Franke, and W. Danysz, "Optical isomers of phenibut inhibit $[\text{H}^3]$ -gabapentin binding in vitro and show activity in animal models of chronic pain," *Pharmacological Reports*, vol. 68, no. 3, pp. 550–554, 2016.
- [8] M. Dambrova, L. Zvejniece, E. Liepinsh et al., "Comparative pharmacological activity of optical isomers of phenibut," *European Journal of Pharmacology*, vol. 583, no. 1, pp. 128–134, 2008.
- [9] E. Vavers, L. Zvejniece, B. Svalbe et al., "The neuroprotective effects of R-phenibut after focal cerebral ischemia," *Pharmacological Research*, vol. 113, pp. 796–801, 2016.
- [10] H. M. Bramlett and W. D. Dietrich, "Pathophysiology of cerebral ischemia and brain trauma: similarities and differences," *Journal of Cerebral Blood Flow & Metabolism*, vol. 24, no. 2, pp. 133–150, 2004.
- [11] Y. Xiong, A. Mahmood, and M. Chopp, "Animal models of traumatic brain injury," *Nature Reviews Neuroscience*, vol. 14, no. 2, pp. 128–142, 2013.
- [12] L. Zvejniece, G. Stelfa, E. Vavers et al., "Skull fractures induce neuroinflammation and worsen outcomes after closed head injury in mice," *Journal of Neurotrauma*, vol. 37, no. 2, pp. 295–304, 2020.
- [13] A. Görlach, K. Bertram, S. Hudcová, and O. Krizanová, "Calcium and ROS: a mutual interplay," *Redox Biology*, vol. 6, pp. 260–271, 2015.
- [14] D. N. Granger and P. R. Kvietys, "Reperfusion injury and reactive oxygen species: the evolution of a concept," *Redox Biology*, vol. 6, pp. 524–551, 2015.
- [15] M. Bains and E. D. Hall, "Antioxidant therapies in traumatic brain and spinal cord injury," *Biochimica et Biophysica Acta*, vol. 1822, no. 5, pp. 675–684, 2012.
- [16] J. T. Weber, "Altered calcium signaling following traumatic brain injury," *Frontiers in Pharmacology*, vol. 3, p. 60, 2012.
- [17] E. D. Hall, R. A. Vaishnav, and A. G. Mustafa, "Antioxidant therapies for traumatic brain injury," *Neurotherapeutics*, vol. 7, no. 1, pp. 51–61, 2010.
- [18] G. Cheng, R. Kong, L. Zhang, and J. Zhang, "Mitochondria in traumatic brain injury and mitochondrial-targeted multipotential therapeutic strategies," *British Journal of Pharmacology*, vol. 167, no. 4, pp. 699–719, 2012.
- [19] M. D'Arco, W. Margas, J. S. Cassidy, and A. C. Dolphin, "The upregulation of $\alpha 2\delta\text{-}1$ subunit modulates activity-dependent Ca^{2+} signals in sensory neurons," *The Journal of Neuroscience*, vol. 35, no. 15, pp. 5891–5903, 2015.
- [20] T. Kinjo, Y. Ashida, H. Higashi et al., "Alleviation by GABAB receptors of neurotoxicity mediated by mitochondrial permeability transition pore in cultured murine cortical neurons exposed to N-methyl-D-aspartate," *Neurochemical Research*, vol. 43, no. 1, pp. 79–88, 2018.
- [21] J. Flygt, K. Ruscher, A. Norberg et al., "Neutralization of interleukin- 1β following diffuse traumatic brain injury in the mouse attenuates the loss of mature oligodendrocytes," *Journal of Neurotrauma*, vol. 35, no. 23, pp. 2837–2849, 2018.
- [22] N. Marklund, "Rodent models of traumatic brain injury: methods and challenges," *Methods in Molecular Biology*, vol. 1462, pp. 29–46, 2016.
- [23] C. Kilkenny, W. Browne, I. C. Cuthill, M. Emerson, D. G. Altman, and NC3Rs Reporting Guidelines Working Group, "Animal research: reporting in vivo experiments: the ARRIVE guidelines," *The Journal of Gene Medicine*, vol. 12, no. 7, pp. 561–563, 2010.
- [24] J. C. McGrath, G. B. Drummond, E. M. McLachlan, C. Kilkenny, and C. L. Wainwright, "Guidelines for reporting experiments involving animals: the ARRIVE guidelines," *British Journal of Pharmacology*, vol. 160, no. 7, pp. 1573–1576, 2010.
- [25] L. Zvejniece, B. Zvejniece, M. Videja et al., "Neuroprotective and anti-inflammatory activity of DAT inhibitor R-phenylpiracetam in experimental models of inflammation in male mice," *Inflammopharmacology*, vol. 28, no. 5, pp. 1283–1292, 2020.
- [26] M. A. Flierl, P. F. Stahel, K. M. Beauchamp, S. J. Morgan, W. R. Smith, and E. Shohami, "Mouse closed head injury model induced by a weight-drop device," *Nature Protocols*, vol. 4, no. 9, pp. 1328–1337, 2009.
- [27] H. Ooigawa, H. Nawashiro, S. Fukui et al., "The fate of Nissl-stained dark neurons following traumatic brain injury in rats: difference between neocortex and hippocampus regarding survival rate," *Acta Neuropathologica*, vol. 112, no. 4, pp. 471–481, 2006.
- [28] R. Hicks, H. Soares, D. Smith, and T. McIntosh, "Temporal and spatial characterization of neuronal injury following lateral fluid-percussion brain injury in the rat," *Acta Neuropathologica*, vol. 91, no. 3, pp. 236–246, 1996.
- [29] M. Makrecka-Kuka, G. Krumschnabel, and E. Gnaiger, "High-resolution respirometry for simultaneous measurement of oxygen and hydrogen peroxide fluxes in permeabilized cells,

- tissue homogenate and isolated mitochondria,” *Biomolecules*, vol. 5, no. 3, pp. 1319–1338, 2015.
- [30] G. Krumschnabel, M. Fontana-Ayoub, Z. Sumbalova et al., “Simultaneous high-resolution measurement of mitochondrial respiration and hydrogen peroxide production,” *Methods in Molecular Biology*, vol. 1264, pp. 245–261, 2015.
- [31] J. Burtscher, L. Zangrandi, C. Schwarzer, and E. Gnaiger, “Differences in mitochondrial function in homogenated samples from healthy and epileptic specific brain tissues revealed by high-resolution respirometry,” *Mitochondrion*, vol. 25, pp. 104–112, 2015.
- [32] M. Makrecka, B. Svalbe, K. Volska et al., “Mildronate, the inhibitor of L-carnitine transport, induces brain mitochondrial uncoupling and protects against anoxia-reoxygenation,” *European Journal of Pharmacology*, vol. 723, pp. 55–61, 2014.
- [33] T. Kristián, J. Gertsch, T. E. Bates, and B. K. Siesjö, “Characteristics of the calcium-triggered mitochondrial permeability transition in nonsynaptic brain mitochondria: effect of cyclosporin A and ubiquinone O,” *Journal of Neurochemistry*, vol. 74, no. 5, pp. 1999–2009, 2000.
- [34] C. P. Baines, R. A. Kaiser, N. H. Purcell et al., “Loss of cyclophilin D reveals a critical role for mitochondrial permeability transition in cell death,” *Nature*, vol. 434, no. 7033, pp. 658–662, 2005.
- [35] T. Kobayashi, S. Kuroda, M. Tada, K. Houkin, Y. Iwasaki, and H. Abe, “Calcium-induced mitochondrial swelling and cytochrome c release in the brain: its biochemical characteristics and implication in ischemic neuronal injury,” *Brain Research*, vol. 960, no. 1-2, pp. 62–70, 2003.
- [36] E. Marais, N. Klugbauer, and F. Hofmann, “Calcium channel $\alpha(2)\delta$ subunits-structure and gabapentin binding,” *Molecular Pharmacology*, vol. 59, no. 5, pp. 1243–1248, 2001.
- [37] N. Qin, S. Yagel, M.-L. Momplaisir, E. E. Codd, and M. R. D’Andrea, “Molecular cloning and characterization of the human voltage-gated calcium channel $\alpha 2\delta$ -4 subunit,” *Molecular Pharmacology*, vol. 62, no. 3, pp. 485–496, 2002.
- [38] A. C. Dolphin, “The $\alpha 2\delta$ subunits of voltage-gated calcium channels,” *Biochimica et Biophysica Acta*, vol. 1828, no. 7, pp. 1541–1549, 2013.
- [39] C. P. Taylor and R. Garrido, “Immunostaining of rat brain, spinal cord, sensory neurons and skeletal muscle for calcium channel $\alpha 2$ -delta ($\alpha 2$ - δ) type 1 protein,” *Neuroscience*, vol. 155, no. 2, pp. 510–521, 2008.
- [40] G. Gurkoff, K. Shahlaie, B. Lyeth, and R. Berman, “Voltage-gated calcium channel antagonists and traumatic brain injury,” *Pharmaceuticals (Basel)*, vol. 6, no. 7, pp. 788–812, 2013.
- [41] C. Calikoglu, H. Aytakin, O. Akgül et al., “Effect of pregabalin in preventing secondary damage in traumatic brain injury: an experimental study,” *Medical Science Monitor*, vol. 21, pp. 813–820, 2015.
- [42] M. Shamsi Meymandi, Z. Soltani, G. Sepehri, S. Amiresmaili, F. Farahani, and M. Moeini Aghataei, “Effects of pregabalin on brain edema, neurologic and histologic outcomes in experimental traumatic brain injury,” *Brain Research Bulletin*, vol. 140, pp. 169–175, 2018.
- [43] K.-Y. Ha, Y.-H. Kim, K.-W. Rhyu, and S.-E. Kwon, “Pregabalin as a neuroprotector after spinal cord injury in rats,” *European Spine Journal*, vol. 17, no. 6, pp. 864–872, 2008.
- [44] K.-Y. Ha, E. Carragee, I. Cheng, S.-E. Kwon, and Y.-H. Kim, “Pregabalin as a neuroprotector after spinal cord injury in rats: biochemical analysis and effect on glial cells,” *Journal of Korean Medical Science*, vol. 26, no. 3, pp. 404–411, 2011.
- [45] J. K. Newcomb, A. Kampfl, R. M. Posmantur et al., “Immunohistochemical study of calpain-mediated breakdown products to alpha-spectrin following controlled cortical impact injury in the rat,” *Journal of Neurotrauma*, vol. 14, no. 6, pp. 369–383, 1997.
- [46] R. M. Posmantur, J. K. Newcomb, A. Kampfl, and R. L. Hayes, “Light and confocal microscopic studies of evolutionary changes in neurofilament proteins following cortical impact injury in the rat,” *Experimental Neurology*, vol. 161, no. 1, pp. 15–26, 2000.
- [47] L. Talley Watts, J. A. Long, J. Chemello et al., “Methylene blue is neuroprotective against mild traumatic brain injury,” *Journal of Neurotrauma*, vol. 31, no. 11, pp. 1063–1071, 2014.
- [48] E. A. Newell, B. P. Todd, J. Mahoney, A. A. Pieper, P. J. Ferguson, and A. G. Bassuk, “Combined blockade of interleukin-1 α and -1 β signaling protects mice from cognitive dysfunction after traumatic brain injury,” *eNEURO*, vol. 5, no. 2, pp. -ENEURO.0385–ENEU17.2018, 2018.
- [49] M. Sun, R. D. Brady, D. K. Wright et al., “Treatment with an interleukin-1 receptor antagonist mitigates neuroinflammation and brain damage after polytrauma,” *Brain, Behavior, and Immunity*, vol. 66, pp. 359–371, 2017.
- [50] N. J. Rothwell and G. N. Luheshi, “Interleukin 1 in the brain: biology, pathology and therapeutic target,” *Trends in Neurosciences*, vol. 23, no. 12, pp. 618–625, 2000.
- [51] K.-T. Lu, Y.-W. Wang, J.-T. Yang, Y.-L. Yang, and H.-I. Chen, “Effect of interleukin-1 on traumatic brain injury-induced damage to hippocampal neurons,” *Journal of Neurotrauma*, vol. 22, no. 8, pp. 885–895, 2005.
- [52] F. Clausen, A. Hånell, M. Björk et al., “Neutralization of interleukin-1 β modifies the inflammatory response and improves histological and cognitive outcome following traumatic brain injury in mice,” *The European Journal of Neuroscience*, vol. 30, no. 3, pp. 385–396, 2009.
- [53] R. Tehranian, S. Andell-Jonsson, S. M. Beni et al., “Improved recovery and delayed cytokine induction after closed head injury in mice with central overexpression of the secreted isoform of the interleukin-1 receptor antagonist,” *Journal of Neurotrauma*, vol. 19, no. 8, pp. 939–951, 2002.
- [54] J. Lazovic, A. Basu, H.-W. Lin et al., “Neuroinflammation and both cytotoxic and vasogenic edema are reduced in interleukin-1 type 1 receptor-deficient mice conferring neuroprotection,” *Stroke*, vol. 36, no. 10, pp. 2226–2231, 2005.
- [55] R. A. Floyd and J. M. Carney, “Free radical damage to protein and DNA: mechanisms involved and relevant observations on brain undergoing oxidative stress,” *Annals of Neurology*, vol. 32, no. S1, pp. S22–S27, 1992.
- [56] C. Werner and K. Engelhard, “Pathophysiology of traumatic brain injury,” *British Journal of Anaesthesia*, vol. 99, no. 1, pp. 4–9, 2007.
- [57] M. Prins, T. Greco, D. Alexander, and C. C. Giza, “The pathophysiology of traumatic brain injury at a glance,” *Disease Models & Mechanisms*, vol. 6, no. 6, pp. 1307–1315, 2013.
- [58] E. E. Genrikhs, E. V. Stelmashook, O. V. Popova et al., “Mitochondria-targeted antioxidant SkQT1 decreases trauma-induced neurological deficit in rat and prevents amyloid- β -induced impairment of long-term potentiation in rat

- hippocampal slices,” *Journal of Drug Targeting*, vol. 23, no. 4, pp. 347–352, 2015.
- [59] J. Zhou, H. Wang, R. Shen et al., “Mitochondrial-targeted antioxidant MitoQ provides neuroprotection and reduces neuronal apoptosis in experimental traumatic brain injury possibly via the Nrf2-ARE pathway,” *American Journal of Translational Research*, vol. 10, no. 6, pp. 1887–1899, 2018.
- [60] R. L. Schmidt and L. L. Lenz, “Distinct licensing of IL-18 and IL-1 β secretion in response to NLRP3 inflammasome activation,” *PLoS One*, vol. 7, no. 9, article e45186, 2012.
- [61] R. L. Veech, C. R. Valeri, and T. B. VanItallie, “The mitochondrial permeability transition pore provides a key to the diagnosis and treatment of traumatic brain injury,” *IUBMB Life*, vol. 64, no. 2, pp. 203–207, 2012.
- [62] D. Huynh, C. S. Wai, A. Liang, T. J. Maher, and A. Pino-Figueroa, “In vitro neuroprotective activity of phenibut,” *The FASEB Journal*, vol. 26, 672.6 pages, 2012.
- [63] V. N. Perfilova, T. A. Popova, I. I. Prokofiev, I. S. Mokrousov, O. V. Ostrovskii, and I. N. Tyurenkov, “Effect of phenibut and glufimet, a novel glutamic acid derivative, on respiration of heart and brain mitochondria from animals exposed to stress against the background of inducible NO-synthase blockade,” *Bulletin of Experimental Biology and Medicine*, vol. 163, no. 2, pp. 226–229, 2017.
- [64] J. T. Cole, A. Yarnell, W. S. Kean et al., “Craniotomy: true sham for traumatic brain injury, or a sham of a sham?,” *Journal of Neurotrauma*, vol. 28, no. 3, pp. 359–369, 2011.
- [65] L. D. Schurman, T. L. Smith, A. J. Morales et al., “Investigation of left and right lateral fluid percussion injury in C57BL6/J mice: in vivo functional consequences,” *Neuroscience Letters*, vol. 653, pp. 31–38, 2017.